Published in final edited form as:
Brain Res. 2005 November 16; 1062(1-2): 63–73.

A detailed characterization of loud noise stress: Intensity analysis of hypothalamo–pituitary–adrenocortical axis and brain activation

Andrew Burow, **Heidi E.W. Day**, and **Serge Campeau***
Department of Psychology and Center for Neuroscience, University of Colorado, Boulder, Muenzinger Bldg., Rm. D244, UCB 345, Boulder, CO 80309, USA

Abstract

The present studies were undertaken to help determine the putative neural circuits mediating activation of the hypothalamo–pituitary–adrenocortical (HPA) axis and the release of adrenocorticotropin hormone (ACTH) and corticosterone in response to the perceived threat of loud noise. This experiment involved placing rats in acoustic chambers overnight to avoid any handling and context changes prior to noise exposure, which was done for 30 min (between 9:00 and 10:00 am) at intensities of 80, 85, 90, 95, 100, 105, and 110 dBA in different groups ($n = 8$), and included a background condition (60 dBA ambient noise). This manipulation produced a noise-intensity-related increase in plasma ACTH and corticosterone levels, with levels beginning to rise at approximately 85 dBA. c-*fos* mRNA induction was very low in the brains of the control and 80 dBA groups, but several brain regions displayed a noise-intensity-related induction. Of these, several forebrain regions displayed c-*fos* mRNA induction highly correlated ($r > 0.70$) with that observed in the paraventricular hypothalamic nucleus and plasma ACTH levels. These regions included the ventrolateral septum, the anteroventral subiculum, several preoptic nuclei, the anterior bed nucleus of the stria terminalis (BNST), the anterior paraventricular nucleus of the thalamus, and the medial subdivision of the medial geniculate body. Together with prior findings with audiogenic stress, the present results suggest that either or both the anterior BNST or the lateral septum is ideally situated to trigger HPA axis activation by stimuli that are potentially threatening.

Keywords

ACTH; Corticosterone; Audiogenic; c-fos; Septum; Bed nucleus of the stria terminalis

1. Introduction

Situations that disturb or are perceived to threaten physiologic homeostasis elicit well-integrated effector responses targeted at restoring balance or in anticipation to such a change. In particular, the endocrine release of glucocorticoids is triggered across a wide range of threat situations and species [53]. These observations suggest that a set of brain regions and circuits control threat-related responses. The paraventricular nucleus of the hypothalamus (PVN) is responsible for activation of the anterior pituitary corticotropes ultimately controlling the production and release of adrenocorticoids [2]. The brain circuits that regulate endocrine release are relatively detailed, especially with regard to physiologic stimuli that directly disturb homeostasis [5–7,23,38,47]. However, different brain regions appear to be associated with perceived threats to homeostasis (variously termed processive, psychological, or emotional stress) without direct and immediate physiologic challenges [11,18,30,34,39,49]. Although redundant proximal effector circuits appear to be responsible for activation of the

* Corresponding author. Fax: +1 303 492 2967. E-mail address: serge.campeau@colorado.edu (S. Campeau).

hypothalamo–pituitary–adrenocortical (HPA) axis to direct physiologic disturbances and perceived threatening situations [19,34,35], an important question remains as to how and which part of the brain mediates perceived threat determination and how this information is passed down to the proximal effector systems engaged by these challenges and in particular the PVN. The present studies were designed to help further characterize putative forebrain circuits associated with HPA axis activation to a perceived threat that does not directly impact physiologic homeostasis.

The use of immediate–early genes (IEGs) such as c-*fos* provides a tool to map putative brain regions that regulate the HPA axis in response to several threat stimuli, in rats (see [37,54] for reviews). Combined with anatomical knowledge of PVN afferents, these stress-induced IEG maps have suggested a number of brain areas that are commonly activated by different perceived threat situations and have been postulated to control HPA axis activation under these conditions. However, the procedures employed during a variety of stress situations have traditionally confounded the specific stressful stimulus with other aspects of the experimental manipulations. In a previous study, attempts were made to control for some of these confounding factors by using a stimulus that could be graded from non-stressful to stressful levels, thus allowing a distinction between brain regions displaying c-*fos* mRNA induction associated with novelty or modality-specific stimulus processing, as compared to those closely associated with the stressful property of the stimulus [8]. Unfortunately, animals were handled shortly prior to the stimulus presentation and even after extensive habituation of the animals to the experimental context (7–10 days of handling and placement in context for 10 min/day), this handling and context change produced c-*fos* mRNA induction in several brain regions on the test day. This outcome precluded a clear association with stress or HPA axis activation given the subtractive process required in analyzing the data. For instance, important regions implicated in stress reactivity such as the medial prefrontal cortex and the hippocampus were not found to be particularly associated with increasing loud noise intensities [8].

The present study was designed to minimize this last problem, while retaining the use of noise intensities from non-stressful to stressful levels, as measured by activation of the HPA axis products adrenocorticotropin hormone (ACTH) and corticosterone, in rats. A more comprehensive range of noise intensities, compared to a prior study [8], were employed to clarify the threshold intensity required to activate the HPA axis. Induction of c-*fos* mRNA was used as a marker of regional brain activity, and this induction was correlated with that observed in the PVN and plasma levels of ACTH and corticosterone.

2. Procedures

A total of 64 Harlan (Indianapolis, IN) male Sprague–Dawley rats, weighing 200–225 g upon arrival to the colony were used. They were housed in a dedicated colony facility and grouped four to five in clear polycarbonate cages (48 × 27 × 20 cm) containing floor wood shavings and covered with wire lids providing food (rat chow) and water ad libitum. They were kept on a controlled light/dark cycle (lights on 7:00 am–off at 7:00 pm), under constant humidity and temperature conditions. Animals were housed for a period of at least 7 days after arrival from the supplier before any experimental manipulations were conducted. They were then handled for a few minutes each day for 5 to 7 days prior to the experimental manipulations. All procedures were performed between 9:00 am and 12:00 pm to reduce variability due to normal circadian hormonal variations. All procedures were reviewed and approved by the Institutional Animal Care and Use Committee of the University of Colorado and conformed to the United States of America NIH Guide for the Care and Use of Laboratory Animals.

2.1. Apparatus

Noise was generated and presented in a different, remote, room from the animal colony, into eight ventilated double wooden (2 cm plywood board) experimental boxes, with the outer box lined internally with 1.5 cm insulation (Celotex™). The internal dimensions of the inner box are 60 (w) × 38 (d) × 38 cm (h), which allows placement of a polycarbonate rat home cage inside. Each enclosure is fitted with a single 15.25 × 22.85 cm Optimus speaker (#12-1769-120 W RMS) fixed in the middle of the ceiling. Lighting is provided by a fluorescent lamp (15 W) located in the upper left corner of the chamber, which is kept on the same cycle as the main colony room. Noise is produced by a General Radio (#1381; West Concord, MA) solid-state random-noise generator with the bandwidth set at 2 Hz–50 kHz. The output of the noise generator is fed to power amplifiers (Model PA-600X-Pyramid Studio Pro; Brooklyn, NY), the outputs of which feed the speakers. Noise intensity is measured by placing a Radio Shack Realistic Sound Level Meter (#33-2050-A scale; Fort Worth, TX) in the rat's home cages at several locations and taking an average of the different readings. The noise level provided by the ventilating fans is approximately 60 dB (sound pressure level-SPL, A scale), which will be referred throughout as the “quiet” or background/ambient noise level. The noise level in the quiet animal colony averages approximately 55 dBA (SPL).

2.2. Behavioral procedures

The behavioral procedures consisted of placing rats ($N = 64$) singly in polycarbonate cages (43 × 22 × 21 cm) containing floor wood shavings and covered with wire lids (with food and water), similar to their home cages. The study was conducted in two cohorts of 32 rats each. They were immediately transported to the remote room and placed into the experimental boxes on the afternoon prior to noise presentation the next morning, to avoid manipulation and transport of the rats immediately prior to noise exposure. Rats were divided into eight groups, with one group simply exposed to the experimental boxes without noise (60 dBA; $n = 8$), while each of the other groups ($n = 8$/group) received a 30-min noise exposure ranging from 80 dBA (SPL) to 110 dBA (SPL), in increments of 5 dBA. Immediately after noise (or the control experimental box) exposure, the rats from the first cohort ($n = 4$/group) were sacrificed by decapitation, trunk blood was collected, and the brains were removed to be later processed for c-*fos* mRNA detection. The rats from the second cohort ($n = 4$/group) were treated identically except that only blood samples sufficient to measure plasma corticosterone were collected. This was performed by quickly removing a rat from the experimental chamber, gently but firmly wrapping them in a clean towel with the tail exposed on a countertop, and making a small incision to one of the lateral tail veins with the corner of a razor blade to obtain approximately 150 μl of blood. The rats were returned within 2 min from removal to their home cages and returned to the colony, as these rats were employed in a continuing chronic noise study. One animal in the 80 dBA group of the first cohort escaped for a brief period before being sacrificed, and its stress hormone levels were among the highest of all groups, in contrast to the levels of the other seven rats in this group, so the data from this subject were excluded and not used for data analysis.

2.3. Corticosterone and ACTH radioimmunoassays

Blood was collected into ice-chilled tubes containing EDTA. Blood samples were centrifuged at 290 *g* for 10 min, the plasma was pipetted into 0.5 ml Ependorf micro-centrifuge tubes, and stored at −80 °C until assayed.

Corticosterone was measured by radioimmunoassay using a specific rabbit antibody (gift from Dr. S. Watson, Univ. Michigan), with less than 3% cross-reactivity with other steroids. Plasma samples were diluted 1:100 in 0.05 M sodium phosphate buffer containing 0.25% bovine serum albumin (BSA) pH 7.4 and corticosterone separated from binding protein by heat (70 °C, 30 min). Duplicate samples of 200 μl to which 50 μl of trace (^{3}H-corticosterone; Amersham 50

Ci/mmol, 10,000 cpm/tube) and 50 μl of corticosterone antibody (final concentration 1:12800) were incubated at 4 °C overnight. Separation of bound from free corticosterone was achieved by adding 0.5 ml of chilled 1% charcoal–0.1% dextran mixture in buffer for 10 min at 4 °C and centrifuged for 10 min at 1800 *g* (Eppendorf/Brinkman 5810 R). The supernatant was poured into 4 ml scintillation fluid and bound ^{3}H-corticosterone counted on a Packard Instruments (Model 1600 TR) liquid scintillation analyzer and compared to a standard curve (range: 0–80 μg/dl). All samples were measured simultaneously to reduce interassay variability; within assay variability was less than 8%.

ACTH was measured with a kit (ACTH 130 T kit-Cat. No. 40-2195; Nichols Institute Diagnostics, San Clemente, CA) according to the manufacturer's protocol. The sensitivity of the assay ranged from 5 to 1400 pg/ml. All samples were measured simultaneously to reduce interassay variability.

2.4. In situ hybridization histochemistry

Brains were sectioned (10 μm) on a cryostat (Leica model 1850, Wetzlar, Germany), thaw mounted onto polylysine coated slides, and stored at −80 °C until further processed. Slides were fixed in a buffered 4% paraformaldehyde solution for 1 h and rinsed in 3 changes of 2× standard saline citrate (SSC) buffer. The slides were then acetylated in 0.1 M triethanolamine containing 0.25% acetic anhydride for 10 min, rinsed for an additional 5 min in distilled H_2O, and dehydrated in a progressive series of alcohols.

^{35}S-labelled cRNA probes were generated for c-*fos* from cDNA subclones in transcription vectors using standard in vitro transcription methodology. The rat c-*fos* cDNA clone (courtesy of Dr. T. Curran, St. Jude Children's Research Hospital, Memphis, TN) was subcloned in pGem3Z and yields a 680 nt cRNA probe. Riboprobes were labeled in a reaction mixture consisting of 1 μg linearized plasmid, 1× T7 or SP6 transcription buffer (Promega), 125 μCi ^{35}S-UTP, 150 μM NTPs (CTP, ATP, and GTP), 12.5 mM dithiothreitol, 20 U RNase inhibitor, and 6 U RNA polymerase (T7). The reactions were allowed to proceed for 120 min at 37 °C, and probes were separated from free nucleotides over a Sephadex G50-50 column. Riboprobes were diluted in hybridization buffer to yield approximately 1–4 × 10^{6} dpm/65 μl buffer. The hybridization buffer consisted of 50% formamide, 10% dextran sulfate, 2× SSC, 50 mM sodium phosphate buffer (pH 7.4), 1× Denhardt's solution, and 0.1 mg/ml yeast tRNA. Diluted probe (65 μl) was applied to each slide, and sections were coverslipped. Slides were placed in sealed plastic boxes lined with filter paper moistened with 50% formamide in distilled water and were subsequently incubated overnight at 55 °C. Coverslips were then removed, and slides were rinsed several times in 2× SSC. Slides were then incubated in RNase A (200 μg/ml) for 60 min at 37 °C, washed successively in 2×, 1×, 0.5×, and 0.1× SSC for 5–10 min each, and washed in 0.1× SSC for 60 min at 70 °C. Slides were subsequently rinsed in fresh 0.1× SSC, dehydrated in a graded series of alcohols, and exposed to Kodak MR X-ray film.

Control experiments were performed on tissue sections pre-treated with RNase A (200 μg/ml at 37 °C for 60 min) prior to hybridization; this treatment prevented labeling. Alternatively, some control sections were hybridized with the sense cRNA strands, which in all cases did not lead to significant hybridization to tissue sections (data not shown).

Importantly, three to five slides (four sections/slide) for a given brain region from each rat included in the study were processed simultaneously to allow direct comparisons of c-*fos* mRNA in the same regions. Multiple in situ hybridizations were thus performed at different levels of the brain with all animals represented to reduce the effects of technical variations within regions. Sections of all rats in the same region were all exposed on the same X-ray film to further minimize variations. Semi-quantitative analyses of c-*fos* mRNA were performed on digitized images from X-ray films in the linear range of the gray values obtained from our

acquisition system (Northern Light lightbox model B95 [Imaging Res. Inc. St. Catharines, Ontario], a SONY TV camera model XC-ST70 fitted with a Navitar 7000 zoom lens [Rochester, NY], connected to an LG3-01 frame grabber [Scion Corp., Frederick, MD] inside a Dell Dimension 500, captured with Scion Image beta rel. 4.02). Signal pixels of a region of interest were defined as being 3.5 standard deviations above the mean gray value of a cell poor area close to the region of interest. The number of pixels and the average pixel values above the set background were then computed for each region of interest and multiplied, giving an integrated mean gray value measure. An average of four to eight measurements were made on different sections (which included bilateral counts made in all cases), for each region of interest, and these values were further averaged to get a single integrated mean gray value per region for each rat. This analytic method gives relative semi-quantitative results that are comparable to doing a quantitative grain analysis on photographic emulsion-dipped sections [17].

The pictures presented in Fig. 2 were obtained by importing the digital images captured with Scion's LG3 frame grabber into Adobe Photoshop (Adobe Systems Inc., Seattle, WA), inverting the image color, and adjusting the brightness/contrast control to achieve a similar black background.

2.5. Statistics

One-way ANOVAs were performed on mean ACTH and corticosterone values ($P = 0.05$). This was followed by Tukey's HSD post hoc multiple means comparisons to determine the intensity at which differences were reliable. One-way ANOVAs were also computed on the mean integrated gray values obtained from each region where c-*fos* mRNA induction was measured ($P = 0.05$). These were followed by Tukey's HSD post hoc multiple means comparisons ($P = 0.05$) to determine more exactly the source of the differences obtained with the initial ANOVAs. Pearson correlation coefficients were computed on the regional brain c-*fos* mRNA data set at all intensities tested and the respective ACTH and corticosterone values. Meaningful correlations were taken to exceed an r value of 0.70, which accounts for approximately 50% of the variance, and in all cases, $P < 0.01$ (two-tailed tests). All statistics were performed using the SPSS for Windows (rel. 11.0.1; Chicago, IL) statistical program.

3. Results

Previous work in our laboratory has shown that c-*fos* mRNA begins to rise quickly but peaks at approximately 30 min in all the brain regions investigated. Based on these results, the sound intensity manipulation was carried out with a 30-min stimulus duration, a time at which levels of plasma ACTH and corticosterone are among their highest (Patz et al., submitted). The plasma corticosterone levels from the two separate cohorts of animals were within 1 μg/dl from each other at all intensities tested, so the two cohorts were pooled for plasma corticosterone analysis. As shown in Fig. 1, plasma corticosterone and ACTH levels varied with noise intensity ($F_{7,55} = 9.27$, $P < 0.0001$, and $F_{7,23} = 3.44$, $P < 0.05$, for corticosterone and ACTH, respectively), with both measures displaying very reliable linear trends (Ps < 0.0001). Corticosterone levels at intensities ≥90 dBA were significantly elevated from both control and 80 dBA groups (Tukey; $P < 0.05$), the latter two being statistically identical (Tukey; $P > 0.05$). The 85 dBA group was not significantly elevated compared to the two lower intensity groups (60 and 80 dBA), or the 95 dBA group, most likely due to the higher variability displayed by the middle intensity groups (85–95 dBA), as can be gathered from the standard errors of the mean (see Fig. 1). Fig. 1 also shows a slightly different intensity-related pattern of ACTH release, as compared to corticosterone. For plasma ACTH, reliable intensity differences were observed between the 60 and 80 dBA groups and the 110 dBA intensity group (Tukey; $P < 0.05$).

Induction of c-*fos* mRNA was virtually absent in the control (60 dBA) condition, accomplishing one of the primary goals for this study (see Fig. 2). Some cortical and thalamic areas did exhibit diffuse induction in the control rats, but this was low compared to the experimental conditions. Areas with moderate c-*fos* mRNA induction in control rats that did not show a systematic increase with noise presentation included the cingulate and piriform cortices and the anterodorsal nucleus of the thalamus. Thus, overnight housing in the experimental apparatus was successful at minimizing c-*fos* mRNA induction in the control condition.

Given the sparse c-*fos* mRNA induction in the control background condition, noise-induced c-*fos* mRNA induction over control levels was widely observed in the regions investigated (see Table 1; reliable *F*s, $P < 0.05$). As seen from Table 1, some regions displayed elevated c-*fos* mRNA in response to 80–85 dB noise, without further increases at higher noise intensities. This was observed in the lateral hypothalamic area, the subparafascicular nucleus, and the superior olivary complex. Table 1 also indicates that many regions displayed increasing levels of c-*fos* mRNA with increasing noise intensities. However, the most interesting pattern of regional activity would exhibit the highest correlation to c-*fos* mRNA induction in the PVN, which itself was highly correlated with plasma ACTH levels (Pearson correlation coefficient: $r = 0.92$—see Table 2). As reported above with the endocrine measures, there was a high degree of individual differences, especially in the 85, 90, and 95 dBA groups. Therefore, it seemed more appropriate to correlate regional c-*fos* mRNA induction with these output measures, especially ACTH, which could be expected to be the most direct “read-out” of HPA axis activity, rather than performing a strict noise intensity-related analysis of c-*fos* mRNA induction. A partial list of correlation coefficients is presented in Table 2, which includes the regions with the highest correlations (≥ 0.70) with PVN c-*fos* mRNA induction, ACTH and corticosterone release, and their intercorrelations with each other (all correlations two-tailed test, $P < 0.01$). The correlations from two additional regions, the dorsal dentate gyrus and the piriform cortex, among several that did not display reliable correlations with c-*fos* mRNA in the PVN or plasma ACTH/corticosterone levels, are presented in Table 2 for comparisons. Regions of highest correlations with PVN c-*fos* mRNA, in decreasing order, included the anteromedial division of the bed nucleus of the stria terminalis, the medial division of the medial geniculate body, the anterior portion of the paraventricular nucleus of the thalamus, the ventrolateral septum, the anteroventral subiculum, several preoptic areas (lateral and medial preoptic areas and medial nucleus), and the anteroventral division of the bed nucleus of the stria terminalis. As Table 2 also conveys, many of these regions were moderately correlated with each other. It is interesting to note that even if plasma ACTH levels appeared to be related to noise intensity, none of the auditory regions analyzed (see Table 1), with the exception of the medial division of the medial geniculate body, displayed correlations higher than 0.69 with ACTH or PVN c-*fos* mRNA levels (for the temporal auditory cortex; data not shown). However, c-*fos* mRNA induction in lower auditory related structures (cochlear nuclei, superior olivary complex, different divisions of the inferior colliculus, medial geniculate body) was highly correlated with each other and with noise intensity ($r \geq 0.73$), with the exception of the temporal auditory cortex ($r = 0.53$; data not shown).

4. Discussion

The main findings of this study indicated that loud noise induces endocrine hormone release in an intensity-dependent manner, with a threshold of approximately 85 dBA. Hormonal release was also found to be closely associated with one index of neural activity, c-*fos* mRNA induction, in the paraventricular nucleus of the hypothalamus, and additional brain regions that may play a role in the biological determination of threat without direct physiologic disturbance. Because loud noise was presented in the absence of handling and environmental context change, from non-stressful to stressful levels, this study provides some of the best evidence for the association of forebrain circuits involved in the evaluation of potential threat, as induced

by loud noise, and offers a unique perspective for the putative role of several brain regions in stress responsiveness for this particular class of situations.

The use of increasing noise intensities from non-stressful to stressful levels revealed intensity-related elevations of ACTH and corticosterone levels, with the background (60 dBA) and 80 dBA conditions showing very low levels, and the levels induced by 110 dBA providing the highest levels. From the curves presented in Fig. 1, white noise intensities of approximately 85 dBA are required to induce the release of ACTH and corticosterone. This is somewhat more intense than the noise intensities reported to produce hypoalgesia [29], although in that particular study, noise was presented together with restraint, which may have sensitized the hypoalgesic response to noise. Plasma ACTH levels followed noise intensities closely, with more intermediate values at low to moderate noise intensities, compared to corticosterone release. In addition, the highest correlations between either plasma ACTH or corticosterone levels to any brain region quantified were found for ACTH levels, again suggesting that in the present study, the plasma levels of ACTH were more closely associated with some regional brain activity, as reflected by c-*fos* mRNA induction. It should be noted that area under the curve assessed at different time points would provide a more accurate determination of hormonal release with noise intensity, as compared to determination from a single time point as performed in the present experiment, especially for corticosterone [16,27].

One aim of this study was to reduce brain c-*fos* mRNA induction in response to handling and placement into the experimental apparatus, so as to more clearly define the effects of increasing loud noise intensities on this response. A few brain regions were found to display maximal c-*fos* mRNA induction in response to noise intensities (80–85 dB) producing little or no HPA axis activation. These regions included the lateral hypothalamus, the thalamic subparafascicular nucleus, and the brainstem superior olivary complex. It is conceivable that these brain regions play a role in novelty detection, as the stimuli were presented to the rats for the first time. Additional studies would be required to determine if repeatedly presented stimuli would affect these regions differentially and, therefore, implicate these regions more closely in novelty detection.

In previous work employing loud noise stress [8], simply handling and placing rats in the experimental apparatus had a significant effect on c-*fos* mRNA induction in areas including several hippocampal and frontal cortical regions, which was not further enhanced by loud noise. Because these regions are repeatedly reported to be associated with stress using measures such as catecholamine [1,26,45] and glutamate release [41,42,57], and c-*fos* induction [15,43,46, 61], it was possible that prior handling and context change maximally induced c-*fos* mRNA, clouding the putative capacity of loud noise to induce c-*fos* mRNA in these regions as well. However, most of these regions still failed to show reliable c-*fos* mRNA induction to *increasing* loud noise levels, which cannot be attributed to high induction in the control or low noise (80 dBA) groups. It is conceivable that relatively small c-*fos* mRNA induction was missed in this study and could perhaps be more easily measured with immediate early genes that are more readily expressed (e.g., ZIF-268, Arc) in the hippocampal formation. Because there were virtually no changes in c-*fos* mRNA induction with increasing levels of noise in the dorsal hippocampus and prefrontal cortex, these regions are unlikely to directly provide the excitatory drive involved in HPA axis activation. It should be noted that other functions that are nearly invariably triggered by experimental manipulations leading to most stress situations such as handling, or changes in contextual environment that are traditionally not controlled with stressors such as restraint, immobilization, forced-swim, and electric shock may account for some of the c-*fos* induction observed by others in these regions [15,43,46,61]. Even with extended habituation to handling and contextual changes (10 days of handling and placing in experimental apparatus for 10 min/day; [8]), c-*fos* mRNA in medial prefrontal cortex and hippocampus is maximally induced by these manipulations, which may argue against a simple

novelty detection function. One interesting possibility is that the hippocampal formation plays a relatively important role in context processing, which would likely be minimally activated by audiogenic stress. Our results suggest that the medial prefrontal areas and hippocampus are not dynamically associated with activation of the HPA axis, and indeed, most experimental results point to the involvement of these regions in *inhibition* of HPA axis functions [3,20, 25,33,44]. The role of these regions might be to provide a more tonic type of inhibition upon several effector response systems or perhaps a more phasic, dynamic inhibitory role at later time points that were missed in the present study. In this regard, a novel finding of the present study was the observation of a very significant c-*fos* mRNA induction in the region of the *anteroventral* subiculum, which, to our knowledge, has not been reported to any stress situation previously. Although this was observed in some of our previous work [12], it was most noticeable at the most anterior levels, which is easy to miss. This observation supports the findings that the ventral hippocampus/subiculum plays a specific and distinct role in stress-induced responses compared to the rest of the hippocampal formation [36]. The anatomical specificity of the localization of cells displaying loud noise-induced c-*fos* mRNA induction in the most anterior tip of the ventral subiculum might explain some of the divergent results reported with the more specific ventral subicular lesions on the regulation of HPA and other responses induced mostly by perceived threat situations [31–33,36,44,58]. It will be important to determine the extent of this particular ventral subicular population displaying c-*fos* mRNA induction to stress, and their specific connection and involvement in forebrain circuits associated with different stress situations.

Several additional brain regions displayed reliable c-*fos* mRNA induction in response to increasing levels of noise, as reported previously [8]. These regions included the anteromedial and anteroventral subdivisions of the bed nucleus of the stria terminalis, the ventral and dorsal caudate/putamen, the ventrolateral septum, the septohypothalamic nucleus, the lateral nucleus of the amygdala, several hypothalamic nuclei (medial and lateral preoptic areas, medial preoptic, ventromedial, supramammillary and paraventricular nuclei), the anterior paraventricular thalamic nucleus, the medial division of the medial geniculate body, the external nucleus of the inferior colliculus, and the cochlear nuclei. Interestingly, c-*fos* mRNA induction in several of these regions was highly correlated with that observed in the paraventricular hypothalamic nucleus, itself closely associated with the observed plasma ACTH levels ($r = 0.92$). This result is important because activity at the level of the paraventricular nucleus should be closely associated with the endocrine measure, on the one end, and with activity in at least one of the regions that projects to it, and might be responsible for providing the signal induced by noise presentation. In that respect, the relatively high correlation obtained between c-*fos* mRNA induction in the paraventricular hypothalamic nucleus and the medial subdivision of the medial geniculate body may provide a link between one auditory-responsive structure and the HPA axis. Although there are demonstrated inputs from the medial subdivision of the medial geniculate body to the parvocellular division of the paraventricular hypothalamic nucleus, this direct anatomical link does not appear to be functionally active during loud noise presentation [9], at least at the intensity of noise employed (105 dBA) in that study. Instead, the medial division of the medial geniculate body projects to many hypothalamic and forebrain regions [28,55] observed to display c-*fos* mRNA induction in response to loud noise [9]. This anatomical association may explain some of the high correlations observed between c-*fos* mRNA induction in the paraventricular hypothalamic nucleus and regions receiving projections from the medial division of the medial geniculate body, that in turn project to the paraventricular nucleus or its dendritic region, such as the anterior medial and ventral subdivisions of the bed nucleus of the stria terminalis, several preoptic nuclei, and the posteroventral lateral septum [9,21,48,56]. In addition, ablation of neurons in the region of the medial division of the medial geniculate body blocks loud noise evoked corticosterone release and c-*fos* mRNA induction in many of the forebrain regions observed to display c-*fos* mRNA induction [10]. Thus, one or several of these synaptic relays

may be important to provide the excitatory input that drives the hypophysiotropic neurons of the paraventricular nucleus of the hypothalamus in response to moderate loud noise stress. Alternatively, activity in these forebrain regions may provide descending activation to brainstem circuits including subregions of the nucleus of the solitary tract, which may in turn be necessary for activation of the hypothalamic paraventricular nucleus [19,34,35].

A systematic analysis of the functional significance of the regions that display high correlations with ACTH release and c-*fos* mRNA induction in the paraventricular nucleus of the hypothalamus with respect to activation of the HPA axis by loud noise is under way. Other studies [14,22,24] suggest that nuclei of the bed nucleus of the stria terminalis may play an important role in this function. In addition, although large septal lesions have been found to increase HPA axis activity in response to stress [50–52], more specific lateral septal lesions can inhibit HPA axis activity in response to different non-physical stressors [59,60]. The medial preoptic region has also been shown to play an excitatory role in HPA axis activation, at least to olfactory stimulation [24]. c-fos mRNA in this region may also reflect thermoregulatory responses observed with various stressors [4,13,40], including loud noise (C.V. Masini and S. Campeau, unpublished observations). It is further conceivable that one or more of these areas coordinate activity in response systems other than the endocrine HPA axis given the relatively widespread pattern of efferents provided by regions such as the anterior bed nuclei of the stria terminalis [21] and lateral septum [48] to regions that control a wide range of autonomic and behavioral functions. In turn, these regions receive a number of cortical afferents that ideally situates them in an integrative position to influence many effector systems based on many types of sensory information that may form the underlying basis for the determination of a specific situation as stressful.

Acknowledgements

Thanks are extended to Dr. Robert Spencer for his comments on an initial version of the manuscript. This work was supported by grants from a Young Investigator Award (SC) from the National Alliance for Research on Schizophrenia and Affective Disorders (NARSAD), National Institute of Mental Health B/START 1R03MH062471 (SC), and National Institute of Mental Health MH065327 (SC).

References

1. Abercrombie ED, Keefe KA, DiFrischia DS, Zigmond MJ. Differential effect of stress on in vivo dopamine release in striatum, nucleus accumbens, and medial frontal cortex. J Neurochem 1989;52:1655–1658. [PubMed: 2709017]
2. Antoni FA. Hypothalamic control of adrenocorticotropin secretion: advances since the discovery of 41-residue corticotropin-releasing factor. Endocr Rev 1986;7:351–378. [PubMed: 3023041]
3. Brake WG, Flores G, Francis D, Meaney MJ, Srivastava LK, Gratton A. Enhanced nucleus accumbens dopamine and plasma corticosterone stress responses in adult rats with neonatal excitotoxic lesions to the medial prefrontal cortex. Neuroscience 2000;96:687–695. [PubMed: 10727787]
4. Briese E, Cabanac M. Stress hyperthermia: physiological arguments that it is a fever. Physiol Behav 1991;49:1153–1157. [PubMed: 1896496]
5. Buller KM, Day TA. Systemic administration of interleukin-1beta activates select populations of central amygdala afferents. J Comp Neurol 2002;452:288–296. [PubMed: 12353224]
6. Buller KM, Smith DW, Day TA. Differential recruitment of hypothalamic neuroendocrine and ventrolateral medulla catecholamine cells by non-hypotensive and hypotensive hemorrhages. Brain Res 1999;834:42–54. [PubMed: 10407092]
7. Buller KM, Smith DW, Day TA. NTS catecholamine cell recruitment by hemorrhage and hypoxia. NeuroReport 1999;10:3853–3856. [PubMed: 10716222]
8. Campeau S, Watson SJ. Neuroendocrine and behavioral responses and brain pattern of c-fos induction associated with audiogenic stress. J Neuroendocrinol 1997;9:577–588. [PubMed: 9283046]
9. Campeau S, Watson SJ. Connections of some auditory-responsive posterior thalamic nuclei putatively involved in activation of the hypothalamo–pituitary–adrenocortical axis in response to audiogenic

stress in rats: an anterograde and retrograde tract tracing study combined with Fos expression. J Comp Neurol 2000;423:474–491. [PubMed: 10870087]

10. Campeau S, Akil H, Watson SJ. Lesions of the medial geniculate nuclei specifically block corticosterone release and induction of c-*fos* mRNA in the forebrain associated with loud noise stress in rats. J Neurosci 1997;17:5979–5992. [PubMed: 9221794]
11. Campeau, S.; Day, HEW.; Helmreich, DL.; Kollack-Walker, S.; Watson, SJ. Principles of psychoneuroendocrinology. In: Nemeroff, CB., editor. Clinics of Psychiatry: Psychoneuroendocrinology. W.B. Saunders Co; Philadelphia: 1998. p. 1-18.
12. Campeau S, Dolan D, Akil H, Watson SJ. c-fos mRNA induction in acute and chronic audiogenic stress: possible role of the orbitofrontal cortex in habituation. Stress 2002;5:121–130. [PubMed: 12186690]
13. Chen X, Herbert J. Regional changes in c-fos expression in the basal forebrain and brainstem during adaptation to repeated stress: correlations with cardiovascular, hypothermic and endocrine responses. Neuroscience 1995;64:675–685. [PubMed: 7715780]
14. Crane JW, Buller KM, Day TA. Evidence that the bed nucleus of the stria terminalis contributes to the modulation of hypophysiotropic corticotropin-releasing factor cell responses to systemic interleukin-1beta. J Comp Neurol 2003;467:232–242. [PubMed: 14595770]
15. Cullinan WE, Herman JP, Battaglia DF, Akil H, Watson SJ. Pattern and time course of immediate early gene expression in rat brain following acute stress. Neuroscience 1995;64:477–505. [PubMed: 7700534]
16. Day HE, Akil H. Evidence that cholecystokinin receptors are not involved in the hypothalamic-pituitary-adrenal response to intraperitoneal administration of interleukin-1beta. J Neuroendocrinol 1999;11:561–568. [PubMed: 10444313]
17. Day HE, Nebel S, Sasse S, Campeau S. Inhibition of the central extended amygdala by loud noise and restraint stress. Eur J Neurosci 2005;21:441–454. [PubMed: 15673443]
18. Dayas CV, Buller KM, Day TA. Neuroendocrine responses to an emotional stressor: evidence for involvement of the medial but not the central amygdala. Eur J Neurosci 1999;11:2312–2322. [PubMed: 10383620]
19. Dayas CV, Buller KM, Day TA. Medullary neurones regulate hypothalamic corticotropin-releasing factor cell responses to an emotional stressor. Neuroscience 2001;105:707–719. [PubMed: 11516835]
20. Diorio D, Viau V, Meaney MJ. The role of the medial prefrontal cortex (cingulate gyrus) in the regulation of hypothalamic–pituitary–adrenal responses to stress. J Neurosci 1993;13:3839–3847. [PubMed: 8396170]
21. Dong HW, Petrovich GD, Watts AG, Swanson LW. Basic organization of projections from the oval and fusiform nuclei of the bed nuclei of the stria terminalis in adult rat brain. J Comp Neurol 2001;436:430–455. [PubMed: 11447588]
22. Dunn JD. Plasma corticosterone responses to electrical stimulation of the bed nucleus of the stria terminalis. Brain Res 1987;407:327–331. [PubMed: 3567648]
23. Ericsson A, Kovacs KJ, Sawchenko PE. A functional anatomical analysis of central pathways subserving the effects of interleukin-1 on stress-related neuroendocrine neurons. J Neurosci 1994;14:897–913. [PubMed: 8301368]
24. Feldman S, Conforti N, Saphier D. The preoptic area and bed nucleus of the stria terminalis are involved in the effects of the amygdala on adrenocortical secretion. Neuroscience 1990;37:775–779. [PubMed: 2247223]
25. Figueiredo HF, Bruestle A, Bodie B, Dolgas CM, Herman JP. The medial prefrontal cortex differentially regulates stress-induced c-fos. Eur J Neurosci 2003;18:2357–2364. [PubMed: 14622198]
26. Finlay J, Zigmond M, Abercrombie E. Increased dopamine and norepinephrine release in medial prefrontal cortex induced by acute and chronic stress: effects of diazepam. Neurosci 1994;64:619–628.
27. Garcia A, Marti O, Valles A, Dal-Zotto S, Armario A. Recovery of the hypothalamic–pituitary–adrenal response to stress. Effect of stress intensity, stress duration and previous stress exposure. Neuroendocrinology 2000;72:114–125. [PubMed: 10971146]

28. Grove EA. Neural associations of the substantia innominata in the rat: afferent connections. J Comp Neurol 1988;277:315–346. [PubMed: 2461972]
29. Helmstetter FJ, Bellgowan PS. Hypoalgesia in response to sensitization during acute noise stress. Behav Neurosci 1994;108:177–185. [PubMed: 8192843]
30. Herman JP, Cullinan WE. Neurocircuitry of stress: central control of the hypothalamo–pituitary–adrenocortical axis. Trends Neurosci 1997;20:78–84. [PubMed: 9023876]
31. Herman J, Cullinan W, Young E, Akil H, Watson S. Selective forebrain fibertract lesions implicate ventral hippocampal structures in tonic regulation of paraventricular nucleus CRH and AVP mRNA expression. Brain Res 1992;592:228–238. [PubMed: 1333341]
32. Herman JP, Cullinan WE, Morano MI, Akil H, Watson SJ. Contribution of the ventral subiculum to inhibitory regulation of the hypothalamo–pituitary–adrenocortical axis. J Neuroendocrinol 1995;7:475–482. [PubMed: 7550295]
33. Herman JP, Dolgas CM, Carlson SL. Ventral subiculum regulates hypothalamo–pituitary–adrenocortical and behavioural responses to cognitive stressors. Neuroscience 1998;86:449–459. [PubMed: 9881860]
34. Herman JP, Figueiredo H, Mueller NK, Ulrich-Lai Y, Ostrander MM, Choi DC, Cullinan WE. Central mechanisms of stress integration: hierarchical circuitry controlling hypothalamo–pituitary–adrenocortical responsiveness. Front Neuroendocrinol 2003;24:151–180. [PubMed: 14596810]
35. Kinzig KP, D'Alessio DA, Herman JP, Sakai RR, Vahl TP, Figueredo HF, Murphy EK, Seeley RJ. CNS glucagon-like peptide-1 receptors mediate endocrine and anxiety responses to interoceptive and psychogenic stressors. J Neurosci 2003;23:6163–6170. [PubMed: 12867498]
36. Kjelstrup KG, Tuvnes FA, Steffenach HA, Murison R, Moser EI, Moser MB. Reduced fear expression after lesions of the ventral hippocampus. Proc Natl Acad Sci U S A 2002;99:10825–10830. [PubMed: 12149439]
37. Kovacs KJ. c-Fos as a transcription factor: a stressful (re)view from a functional map. Neurochem Int 1998;33:287–297. [PubMed: 9840219]
38. Larsen P, Mikkelsen J. Functional identification of central afferent projections conveying information of acute “stress” to the hypothalamic paraventricular nucleus. J Neurosci 1995;15:2609–2627. [PubMed: 7536817]
39. Li HY, Ericsson A, Sawchenko PE. Distinct mechanisms underlie activation of hypothalamic neurosecretory neurons and their medullary catecholaminergic afferents in categorically different stress paradigms. Proc Natl Acad Sci U S A 1996;93:2359–2364. [PubMed: 8637878]
40. Long NC, Vander AJ, Kluger MJ. Stress-induced rise of body temperature in rats is the same in warm and cool environments. Physiol Behav 1990;47:773–775. [PubMed: 2385651]
41. Lowy MT, Wittenberg L, Yamamoto BK. Effect of acute stress on hippocampal glutamate levels and spectrin proteolysis in young and aged rats. J Neurochem 1995;65:268–274. [PubMed: 7790870]
42. Moghaddam B. Stress activation of glutamate neurotransmission in the prefrontal cortex: implications for dopamine-associated psychiatric disorders. Biol Psychiatry 2002;51:775–787. [PubMed: 12007451]
43. Morrow BA, Elsworth JD, Lee EJ, Roth RH. Divergent effects of putative anxiolytics on stress-induced fos expression in the mesoprefrontal system of the rat. Synapse 2000;36:143–154. [PubMed: 10767061]
44. Nettles KW, Pesold C, Goldman MB. Influence of the ventral hippocampal formation on plasma vasopressin, hypothalamic–pituitary–adrenal axis, and behavioral responses to novel acoustic stress. Brain Res 2000;858:181–190. [PubMed: 10700613]
45. Nisenbaum L, Zigmond M, Sved A, Abercrombie E. Prior exposure to chronic stress results in enhanced synthesis and release of hippocampal norepinephrine in response to a novel stressor. J Neurosci 1991;11:1478–1484. [PubMed: 1674004]
46. Ostrander MM, Richtand NM, Herman JP. Stress and amphetamine induce Fos expression in medial prefrontal cortex neurons containing glucocorticoid receptors. Brain Res 2003;990:209–214. [PubMed: 14568346]
47. Rinaman L. Interoceptive stress activates glucagon-like peptide-1 neurons that project to the hypothalamus. Am J Physiol 1999;277:R582–R590. [PubMed: 10444567]

48. Risold PY, Swanson LW. Connections of the rat lateral septal complex. Brain Res Rev 1997;24:115–195. [PubMed: 9385454]
49. Sawchenko PE, Li HY, Ericsson A. Circuits and mechanisms governing hypothalamic responses to stress: a tale of two paradigms. Prog Brain Res 2000;122:61–78. [PubMed: 10737051]
50. Seggie J. Differential responsivity of corticosterone and prolactin to stress following lesions of the septum or amygdala: implications for psychoneuroendocrinology. Prog Neuro-Psychopharmacol Biol Psychiatry 1987;11:315–324.
51. Seggie J, Shaw B, Uhlir I, Brown GM. Baseline 24-hour plasma corticosterone rhythm in normal, sham-operated and septally-lesioned rats. Neuroendocrinology 1974;15:51–61. [PubMed: 4850733]
52. Seggie J, Uhlir I, Brown GI. Adrenal responses following septal lesions in the rat. Neuroendocrinology 1974;16:225–236. [PubMed: 4476058]
53. Selye, H. The Stress of Life. McGraw-Hill; New York: 1956.
54. Senba E, Ueyama T. Stress-induced expression of immediate early genes in the brain and peripheral organs of the rat. Neurosci Res 1997;29:183–207. [PubMed: 9436645]
55. Simerly RB, Swanson LW. The organization of neural inputs to the medial preoptic nucleus of the rat. J Comp Neurol 1986;246:312–342. [PubMed: 3517086]
56. Simerly RB, Swanson LW. Projections of the medial preoptic nucleus: a *Phaseolus vulgaris* leucoagglutinin anterograde tract-tracing study in the rat. J Comp Neurol 1988;270:209–242. [PubMed: 3259955]
57. Steciuk M, Kram M, Kramer GL, Petty F. Immobilization-induced glutamate efflux in medial prefrontal cortex: blockade by (+)-Mk-801, a selective NMDA receptor antagonist. Stress 2000;3:195–199. [PubMed: 10938580]
58. Tuvnes FA, Steffenach HA, Murison R, Moser MB, Moser EI. Selective hippocampal lesions do not increase adrenocortical activity. J Neurosci 2003;23:4345–4354. [PubMed: 12764123]
59. Usher DR, Lamble RW. ACTH synthesis and release in septallesioned rats exposed to air shuttle-avoidance. Physiol Behav 1969;4:923–927.
60. Usher DR, Kasper P, Birmingham MK. Comparison of pituitary–adrenal function in rats lesioned in different areas of the limbic system and hypothalamus. Neuroendocrinology 1967;2:157–174.
61. Yokoyama C, Sasaki K. Regional expressions of Fos-like immunoreactivity in rat cerebral cortex after stress; restraint and intraperitoneal lipopolysaccharide. Brain Res 1999;816:267–275. [PubMed: 9878776]

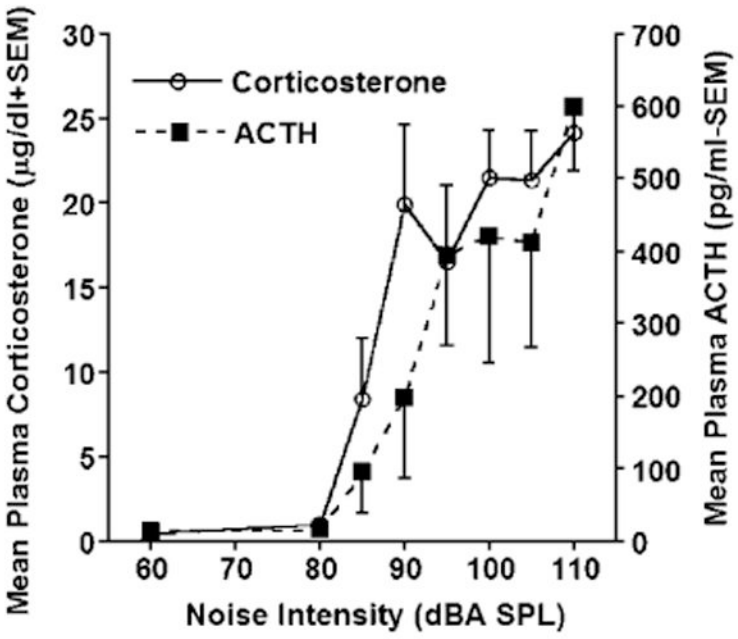

Fig. 1.

Mean levels of plasma corticosterone (μg/dl +SEM) and ACTH (pg/ml −SEM) following 30 min. of white noise presentation at intensities of 80, 85, 90, 95, 100, 105, or 110 dB (A scale, SPL). The 60 dBA group was not exposed to any noise presentation (ambient background noise). 85 dBA was the first intensity to evoke the release of plasma corticosterone and ACTH, and the levels of both hormones rose with increasing intensities, with the highest levels observed at 110 dBA.

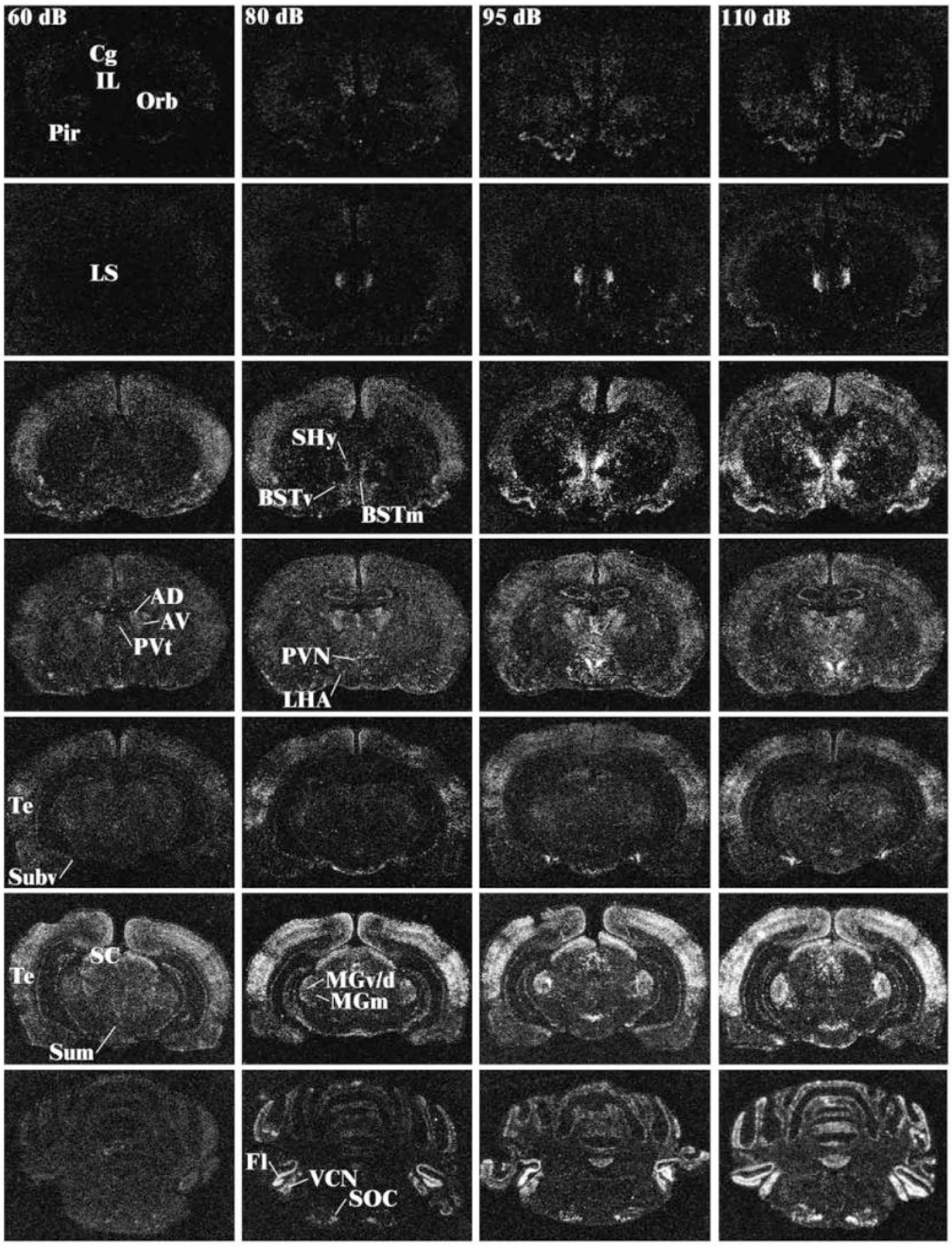

Fig. 2.

Representative photomicrographs of c-*fos* mRNA induction at different levels of the neuraxis for rats in the background noise condition (60 dB—far left column), 80 dB noise (middle left column), 95 dB (middle right column), and 110 dB (far right column). The different levels from top to bottom represent anterior to posterior brain sections. Note the increase in c-*fos* mRNA levels with increasing noise intensities in several brain regions. Abbreviations: AD, anterodorsal thalamic nucleus; AV, anteroventral thalamic nucleus; CG, cingulate cortex; BSTm, anteromedial bed nucleus of the stria terminalis; BSTv, anteroventral bed nucleus of the stria terminalis; IL, infralimbic cortex; Fl, flocculus; MGm, medial division of the medial geniculate body; MGv/d, ventral/dorsal divisions of the medial geniculate body; LHA, lateral

hypothalamic area; LS, lateral septum; Orb, orbitofrontal cortex; Pir, piriform cortex; PVN, paraventricular nucleus of the hypothalamus; PVt, anterior paraventricular nucleus of the thalamus; SC, superior colliculus; SHy, septohypothalamic nucleus; SOC, superior olivary complex; Subv, anteroventral subiculum; Sum, supramammillary nucleus of the hypothalamus; Te, temporal (auditory) cortex; VCN, ventral cochlear nucleus.

Table 1

Semi-quantitative measurement of c-*fos* mRNA induction in various brain regions across varying intensities of noise, reported as mean integrated gray values (/100 ± SEM)

Brain region	Control	80 dB	85 dB	90 dB	95 dB	100 dB	105 dB	110 dB
Forebrain								
BNST medial*	0.9 (0.3)	8.3 (1.6)[a]	36 (6)[a]	51 (7)[b]	89 (8)[b]	103 (11)[b]	134 (13)[b]	167 (15)[b]
BNST ventral*	2.3 (1.0)	5.0 (1.7)[a]	13 (5)[a]	24 (8)[b]	46 (18)[b]	79 (25)[c]	91 (23.4)[c]	64 (8)[b]
Caudate nucleus dor*	3.3 (0.9)	14 (2)[a]	31 (15)[a]	43 (10)[b]	69 (6)[b]	111 (18)[c]	87 (23)[b]	130 (24)[c]
Caudate nucleus ven*	1.2 (0.4)	2.9 (1.1)	6.4 (4.7)[a]	6.8 (2.0)[a]	13 (2)[b]	13 (0.3)[b]	15 (3)[b]	30 (4)[c]
Medial septum	0.6 (0.3)	2.3 (1.4)	1.0 (0.4)	3.5 (1.8)	2.3 (1.1)	4.8 (2.1)	4.6 (1.2)	5.7 (2.6)
Ventrolateral septum*	8.3 (2.1)	18 (5)	87 (20)[a]	125 (78)[b]	598 (181)[c]	527 (125)[c]	497 (101)[c]	578 (113)[c]
Septohypothal. nuc*	4.6 (2.6)	8.3 (1.6)[a]	37 (6)[a]	52 (7)[b]	498 (81)[b]	517 (149)[b]	453 (98)[b]	503 (54)[b]
Amygdala								
Central nucleus	0.9 (0.2)	2.7 (1.5)	2.1 (1.0)	3.1 (1.9)	1.2 (0.6)	3.4 (1.2)	3.1 (0.9)	2.7 (1.5)
Basolateral nucleus	0.8 (0.1)	1.7 (0.4)	5.1 (2.3)	1.3 (0.2)	2.9 (1.0)	2.3 (0.8)	5.4 (2.1)	2.9 (1.2)
Lateral nucleus*	1.2 (0.6)	4.5 (2.1)[a]	7.1 (3.2)[a]	11 (4)[a]	27 (7)[b]	14 (3)[a]	17 (3)[b]	21 (4)[b]
Medial nucleus	1.1 (0.4)	3.1 (0.9)	2.5 (1.0)	6.9 (2.8)	6.8 (2.1)	5.5 (1.2)	7.3 (3.2)	6.4 (2.0)
Hippocampus								
CA1 (dorsal)	0.7 (0.2)	3.9 (1.7)	3.4 (1.6)	2.3 (0.5)	3.7 (0.7)	5.3 (1.0)	4.0 (0.7)	5.0 (1.0)
CA3 (dorsal)	7.4 (2.9)	14 (2.8)	9.4 (3.0)	13 (2.8)	12 (4.3)	18 (3.6)	19 (4.0)	16 (3.9)
Dentate gyrus (dorsal)	6.3 (0.4)	6.8 (1.7)	6.6 (2.5)	7.8 (1.9)	6.8 (0.5)	7.7 (1.1)	8.2 (1.1)	8.8 (1.4)
Subiculum dorsal*	6.1 (1.2)	10 (2)	8.1 (1.3)	10 (3)	17 (5)[a]	23 (4)[a]	12 (1)	19 (3)[a]
Subiculum anteroventral*	2.7 (0.8)	5.2 (1.1)	4.6 (0.7)	46 (5)[b]	63 (19)[b]	76 (11)[b]	59 (4)[b]	73 (8)[b]
Cortex								
Frontal	0.7 (0.2)	2.0 (0.2)	7.5 (3.7)	7.4 (1.3)	7.6 (2.3)	16 (4.6)	7.5 (2.8)	9.6 (5.2)
Infralimbic	0.6 (0.1)	8.7 (6.7)	8.4 (4.3)	20 (8.2)	12 (2.4)	34 (14)	17 (5.5)	30 (11)
Orbital	1.9 (0.9)	8.7 (3.0)	20 (4.4)	32 (14)	19 (4.3)	34 (6.5)	30 (10)	25 (12)
Cingulate*	26 (5)	37 (9)	45 (12)	38 (4)	35 (7)	57 (4)[a]	47 (3)	61 (4)[a]
Piriform	27 (8)	31 (9)	42 (5)	36 (7)	59 (12)	71 (21)	31 (18)	50 (15)
Auditory*	16 (7)	162 (73)	167 (63)	365 (146)	227 (39)	477 (97)	466 (195)	494 (58)[a]
Hypothalamus								
Dorsomedial nucleus	0.5 (0.4)	4.2 (1.1)	7.6 (3.5)	12 (4)	12 (2)	34 (9)	24 (14)	17 (9)
Lateral area*	3.7 (1.2)	12 (2)	27 (6)[a]	13 (4)	12 (5)	21 (5)[a]	13 (2)	29 (4)[a]
Lateral preoptic area*	1.4 (0.4)	13 (2)[a]	18 (3)[a]	27 (5)[b]	81 (13)[c]	78 (15)[c]	89 (12)[c]	112 (17)[c]
Medial preoptic area*	2.5 (0.5)	11 (3)[a]	27 (4)[a]	56 (8)[b]	48 (10)[b]	112 (37)[c]	164 (31)[c]	135 (29)[c]
Medial preoptic nuc*	2.6 (1.4)	6.0 (1.2)	12 (3)[a]	37 (11)[b]	26 (8)[a]	71 (18)[b]	95 (12)[c]	115 (19)[c]
Paraventricular nuc*	1.1 (0.5)	15 (12)[a]	31 (10)[a]	56 (27)[b]	112 (41)[b]	125 (32)[b]	110 (23)[b]	161 (23)[c]
Supramammillary nuc*	0.7 (0.3)	3.0 (1.4)[a]	21 (12)	35 (17)[b]	27 (8)	75 (26)[c]	98 (26)[c]	126 (34)[c]
Ventromedial nucleus*	0.3 (0.1)	1.2 (0.5)[a]	1.5 (0.8)[a]	2.4 (0.9)[a]	10 (3)[c]	15 (3)[c]	12 (3)[c]	8.6 (3.0)[c]
Thalamus								
Anterodorsal nucleus	9.0 (4.4)	12 (3)	24 (14)	30 (6)	20 (6)	32 (12)	25 (7)	29 (9)
Anteroventral nucleus	2.4 (1.0)	7.2 (2.7)	21 (7)	26 (5)	19 (10)	27 (8)	25 (8)	30 (8)
Central nuclei	1.5 (0.4)	10 (3)	20 (7)	13 (4)	24 (12)	31 (7)	21 (6)	35 (10)
Lateral genic. body	43 (12)	84 (26)	79 (13)	109 (24)	136 (31)	107 (37)	78 (14)	121 (38)
Medial genic. med*	6.8 (2.6)	14 (3)	27 (7)	21 (4)	94 (12)[c]	74 (5)[c]	64 (9)[b]	93 (7)[c]
Medial genic. ven/dor*	35 (8)	161 (34)[a]	246 (56)[a]	359 (111)[b]	412 (117)[b]	482 (59)[b]	476 (102)[b]	524 (97)[b]
Ant. Paraventricular nuc*	3.2 (1.3)	12 (4)[a]	23 (9)[a]	16 (4)[a]	45 (17)[c]	61 (9)[c]	49 (13)[c]	62 (12)[c]
Subparafasicular nuc*	0.3 (0.1)	22 (6)[a]	29 (7)[a]	20 (8)[a]	25 (9)[a]	55 (13)[a]	38 (69)[a]	33 (5)[a]
Midbrain, pons, brainstem								
Cochlear nuclei*	9 (4)	142 (56)[a]	193 (26)[a]	298 (25)[a]	346 (17)[b]	376 (103)[b]	494 (140)[b]	491 (93)[c]
Inferior coll. cen/dor*	153 (17)	413 (47)[a]	534 (68)[a]	649 (62)[a]	728 (42)[b]	768 (79)[b]	814 (94)[b]	886 (164)[b]
Inferior coll. ext*	54 (7)	118 (27)[a]	109 (34)[a]	174 (53)[a]	176 (39)[a]	246 (34)[b]	299 (71)[b]	342 (53)[c]

Brain region	Control	80 dB	85 dB	90 dB	95 dB	100 dB	105 dB	110 dB
Sup. olivary complex*	21 (4)	146 (27)[a]	179 (13)[a]	191 (43)[a]	263 (34)[a]	323 (86)[a]	352 (43)[a]	403 (51)[a]
Locus coeruleus*	0.4 (0.1)	1.1 (0.5)	2.1 (0.3)	1.2 (0.4)	3.6 (0.5)[a]	2.8 (0.3)[a]	1.5 (0.2)	2.6 (0.2)
Superior colliculus*	13 (4)	127 (32)[a]	58 (16)[a]	184 (36)[a]	259 (72)[a]	231 (58)[a]	296 (87)[b]	342 (46)[b]
Cerebellum								
Flocculus/paraflocc.*	84 (23)	390 (106)[a]	461 (183)[a]	645 (106)[a]	817 (94)[b]	903 (148)[b]	916 (152)[b]	1104 (114)[b]

Notes to Table 1:

[a] Significantly different from Control group (Tukey, $P < 0.05$).

[b] Significantly different from Control and 80 dB groups (Tukey, $P < 0.05$).

[c] Significantly different from Control, 80, 85 and 90 dB groups (Tukey, $P < 0.05$).

* ANOVA results are significant ($P < 0.05$).

Table 2

Pearson correlation coefficients showing the highest correlations between c-*fos* mRNA induction in the paraventricular nucleus of the hypothalamus and plasma ACTH and corticosterone levels and c-*fos* mRNA induction in other quantified regions

Regions	LSv	Subv	DGd	LPOA	MPOA	MPON	MGm	BSTm	BSTv	PVt	Pir	PVN	ACTH	Cort
LSv	1.0													
Subv	0.68	1.0												
DGd	0.07	0.20	1.0											
LPOA	0.73	0.71	0.34	1.0										
MPOA	0.61	0.63	0.29	0.68	1.0									
MPON	0.60	0.68	0.29	0.74	0.90	1.0								
MGm	0.79	0.81	0.12	0.83	0.63	0.65	1.0							
BSTm	0.81	0.68	0.19	0.72	0.88	0.82	0.79	1.0						
BSTv	0.75	0.63	0.32	0.70	0.68	0.62	0.67	0.74	1.0					
PVt	0.67	0.72	0.13	0.67	0.70	0.70	0.78	0.76	0.63	1.0				
Pir	0.18	0.36	0	0.21	0.12	0.11	0.28	0.14	0.07	0.18	1.0			
PVN	0.80	0.79	0.25	0.77	0.79	0.78	0.84	0.91	0.72	0.83	0.17	1.0		
ACTH	0.80	0.68	0.25	0.70	0.78	0.77	0.77	0.89	0.72	0.71	0.21	0.92	1.0	
Cort	0.86	0.75	0.15	0.69	0.65	0.64	0.80	0.78	0.73	0.63	0.19	0.83	0.82	1.0

Examples of correlations are also given for a few regions (dorsal dentate gyrus and piriform cortex) that displayed no reliable correlations with c-*fos* mRNA in the PVN or ACTH/Cort plasma levels. Other interregional correlations are also presented. Abbreviations: ACTH, adrenocorticotropin hormone; BSTm, anteromedial division of the bed nucleus of the stria terminalis; BSTv, anteroventral division of the bed nucleus of the stria terminalis; Cort, Corticosterone; DGd, dorsal dentate gyrus; LSv, ventrolateral septum; LPOA, lateral preoptic area; MPOA, medial preoptic area; MPON, medial preoptic nucleus; MGm, medial division of the medial geniculate body; Pir, Piriform cortex; PVN, paraventricular nucleus of the hypothalamus; PVt, anterior paraventricular nucleus of the thalamus; Subv, anteroventral subiculum.

All correlations are significant (two-tailed test, $P < 0.01$), except for piriform cortex and dorsal dentate gyrus, which did not reach statistical significance between any of the measures displayed.